Harmonics generation and intense terahertz radiation from polar molecules at multiphoton resonant excitation in laser fields

H. K. Avetissian,* B. R. Avchyan, and G. F. Mkrtchian

Centre of Strong Field Physics, Yerevan State University, 1 A. Manukian, Yerevan 0025, Armenia

(Dated: June 14, 2011)

The coherent radiation spectrum of two-level polar molecules with UV transition is studied at the multiphoton resonant excitation by a moderately strong laser field. The spectrum corresponding to harmonic generation and low-frequency radiation is investigated both analytically and numerically. Specifically, a mechanism for generation of intense smoothly tunable terahertz radiation by two-level molecular configurations (with dynamic Stark shifts) possessing permanent dipole moments, is considered.

PACS numbers: 42.50.Hz, 42.65.Ky, 32.50.+d, 82.53.Kp

I. INTRODUCTION

The interaction of strong (moderately) laser radiation with the matter produces a number of significant processes that include the harmonic generation. The latter is of particular interest because of importance and potential applications of tunable, coherent, intense high-frequency radiation. Generation of high-order laser harmonics is a well-approbated process in the systems composed by atoms or small molecules and modeled most successfully by a "three-step recollision" physical picture [1, 2]. The three-step theoretical models for high harmonic generation does not include any participation of excited bound states in the emission of high harmonics and is essentially valid for harmonics with energy well above the ionization energy [1].

On the other hand, various studies have shown that for the certain systems such as quantum wells and large molecules [3, 4], bound-bound transitions are more important for harmonic generation than the coupling between the ground and the continuum state [5]. This mechanism of harmonic generation without ionization can not provide high-frequency radiation, e.g. x-ray, but can be more efficient for generation of moderately high harmonics, in particular, for UV/VUV applications [6]. For description of strong light scattering process via bound-bound transitions, resonant interaction is of interest. Apart from its pure theoretical interest as a simple model, the resonant interaction regime may allow to increase considerably the efficiency of frequency conversion.

Harmonic generation by a resonantly driven two-level atom has been studied in [7]. However, a two-level atomic system meets difficulties since the required for efficient multiphoton resonant excitation laser fields are so strong that many atomic levels and continuum will play important role [8]. So, two-level atomic system is not a good quantitative model for description of atomic response in case of multiphoton-resonant excitation.

Nevertheless, in some atomic and especially molecular systems one can avoid the difficulties with efficient multiphoton excitation based on the two-level model. As it has been shown [9–14], the multiphoton resonant excitation of a quantum system subjected to a strong laser field is effective when the quantum system has permanent dipole moments (PDM) in the stationary states. Otherwise, the energies of the excited states of a three-level atom should be close enough to each other and the transition dipole moment between these states must be nonzero. Furthermore, these systems have an advantage, which allow to generate radiation with frequency much lower than laser frequency [15, 16]. The effects of diagonal dipole elements on harmonic generation at the one-photon resonance has been considered in [17]. However, for efficient generation of moderately high harmonics by optical pulses one should consider systems with the bound-bound UV/VUV transitions and, therefore, the multiphoton resonant interaction regime is of special interest. The coherent scattering spectrum of a two-level system possessing PDM at multiphoton resonant excitation has been considered in Ref. [18]. However, the presented in this paper analytical results for radiation spectrum have only qualitative character, in the meantime, the numerical calculations have been performed for such strong fields which break the condition of multiphoton resonant excitation (see below Eq. (13)) and also could lead to detrimental ionization in real atomic/molecular systems.

In the present paper, coherent light scattering by two-level polar molecules at multiphoton resonant excitation in the field of a moderately strong laser radiation is investigated. It is shown that the study of this process is important for efficient population transfer, generation of moderately high harmonics, as well as for generation of low-frequency radiation, specifically, for realization of intense smoothly tunable terahertz radiation sources. A simple analytic expression for the time-dependent mean dipole moment, taking into account the dynamic Stark shifts, is obtained. In particular, based on this expression results, concerning the main spectral characteristics of considering process, are in good agreement with results of performed numerical calculations. The effect of compensation of dynamic Stark shift on the radiation spectrum is considered. We compare the spectra of two-level

systems with and without PDM and show the advantages of polar systems for efficient generation of desirable radiation. Special attention is paid to generation of coherent low-frequency radiation in such systems, particularly, smoothly tunable, intense terahertz radiation.

It should be noted that the obtained results may be interesting for different type coherent light sources, such as polar gases, certain organic crystals or quantum dots and etc. [15, 19–22]. Besides, all presented results can be scaled to other systems and diverse domains of the electromagnetic spectrum.

The paper is organized as follows: in Sec. II we present the analytical model and derive the coherent contribution to the harmonic and low-frequency spectra. In Sec. III we present some results of numerical calculations of the considered issue without multiphoton resonant approximation and compare the obtained spectra with analytical results. Finally, conclusions are given in Sec. IV.

II. THEORY

A. Basic Model

We consider a two-level quantum system possessing PDM driven by a time-dependent, intense laser field. The Hamiltonian describing the interaction of the laser field with the considered quantum system is given within semiclassical dipole approximation by

$$\hat{H} = (\varepsilon_1 + V_{11}) |1\rangle\langle1| + (\varepsilon_2 + V_{22}) |2\rangle\langle2|$$
$$+ (V_{12}|1\rangle\langle2| + \text{h.c.}) . \quad (1)$$

Here, ε_1 and ε_2 are the energies of the stationary states $|1\rangle$ and $|2\rangle$ of unperturbed molecule, $\varepsilon_2 > \varepsilon_1$. In Eq. (1)

$$V_{\eta\nu} = -d_{\eta\nu} E_0 \cos \omega_0 t, \quad (2)$$

is the interaction part of Hamiltonian with real matrix element of the electric dipole moment projection $d_{\eta\nu} = \hat{\mathbf{e}} \cdot \mathbf{d}_{\eta\nu}$, and pump wave field is taken to be linearly polarized, with unit polarization vector $\hat{\mathbf{e}}$, slowly varying amplitude E_0, and carrier frequency ω_0. The diagonal terms in (2) describe the interaction due to the PDM and are crucial for effective multiphoton coupling.

The technique which we employ in our calculations has been described earlier in [6]. First we obtain dynamic wave function of the system in the pump laser field, i.e., the solution of the time-dependent Schrödinger equation with Hamiltonian (1). From these solution we deduce formula for expectation value of the time-dependent dipole-moment operator. Note that dipole-moment form of radiation spectrum gives similar results with dipole-acceleration and dipole-velocity forms in case of long pulses [23].

We consider Schrödinger equation:

$$i\frac{\partial |\Psi(t)\rangle}{\partial t} = \hat{H} |\Psi(t)\rangle , \quad (3)$$

with Hamiltonian (1) at multiphoton resonant excitation regime and assume that $|\delta_n| \ll \omega_0$, where δ_n is the n-photon resonance detuning, given by the relation:

$$\delta_n = \varepsilon_1 - \varepsilon_2 + n\omega_0. \quad (4)$$

Here and below, unless stated otherwise, we employ atomic units ($\hbar = e = m_e = 1$). Our method of solving (3) has been described in detail in [10] and will not be repeated here. Under the generalized rotating wave approximation, the time-dependent wave function can be expanded as:

$$|\Psi(t)\rangle = e^{-i\varepsilon_1 t} \{[\overline{a}_1(t) + \alpha_1(t)] |1\rangle + [\overline{a}_2(t) + \alpha_2(t)]$$
$$\times \left[\exp[-i(n\omega_0 t + \int_0^t (V_{22} - V_{11})dt)] \right] |2\rangle \} , \quad (5)$$

where $\overline{a}_i(t)$ are the time-averaged probability amplitudes and $\alpha_i(t)$ are rapidly changing functions over pump wave period. The time-averaged amplitudes $\overline{a}_i(t)$ are:

$$\overline{a}_i = \sum_{j=1}^{2} C_{ij} \exp(i\lambda_j t), \quad (6)$$

where C_{ij} are the constants of integration determined by the initial conditions, and the factors λ_j are the solutions of the second-order characteristic equation:

$$\left\| \begin{matrix} \Delta_n - \lambda & -F_n \\ -F_n & -\Delta_n - \delta_n - \lambda \end{matrix} \right\| = 0, \quad (7)$$

with the function:

$$F_n = \frac{d_{12}}{d_p} n\omega_0 J_n (Z) , \quad (8)$$

and detuning:

$$\Delta_n = \omega_0 \left(\frac{d_{12}}{d_p} \right)^2 \sum_{k \neq n} \frac{k^2 J_k^2 (Z)}{k - n}. \quad (9)$$

Here $d_p = d_{22} - d_{11}$ (let $d_p > 0$) is the difference of PDM in two stationary states -in the excited and ground states. The argument of the ordinary Bessel function $J_n (Z)$ is the difference of dipole interaction energies in units of the pump wave photon energy: $Z = d_p E_0/\omega_0$. The terms F_n and Δ_n describe the resonant coupling and dynamic Stark shift at n-photon resonance, respectively. In deriving these equations we have applied well-known expansion of exponent through Bessel functions with real arguments [24]:

$$e^{iZ \sin \alpha} = \sum_{s=-\infty}^{\infty} J_s (Z) e^{is\alpha}. \quad (10)$$

Assuming smooth turn-on of the pump wave, the relation between the rapidly and slowly oscillating parts of the probability amplitudes can be written as:

$$\alpha_1(t) = \overline{a}_2(t)\frac{d_{12}}{d_p} \sum_{k \neq n} \frac{kJ_k (Z) e^{i(k-n)\omega_0 t}}{k - n}, \quad (11)$$

$$\alpha_2(t) = -\overline{a}_1(t)\frac{d_{12}}{d_p}\sum_{k\neq n}\frac{kJ_k\left(Z\right)e^{-i(k-n)\omega_0 t}}{k-n}. \qquad (12)$$

It should be noted that the nonperturbative resonant approach used here put the following restrictions:

$$|F_n|,|\Delta_n|,|\delta_n| \ll \omega_0 \qquad (13)$$

on the characteristic parameters of the considered problem (for more details see [10]). As it was mentioned in Introduction, this condition is not fulfilled in Ref. [18].

B. Harmonic generation

We restrict our study to the coherent part of the spectrum, i.e., the spectrum of the mean dipole moment which is predominant for the forward direction when the number of scatterers is relatively large [25, 26]. In the Schrödinger picture the coherent part of the spectrum is [25]:

$$S(\omega) = \left|\int_{-\infty}^{\infty}dt e^{-i\omega t}\left\langle D(t)\right\rangle\right|^2, \qquad (14)$$

where

$$\left\langle D(t)\right\rangle = \left\langle\Psi(t)\right|\hat{\mathbf{e}}\cdot\hat{\mathbf{d}}(\mathbf{0})\left|\Psi(t)\right\rangle, \qquad (15)$$

is the time-dependent mean dipole moment, which is the main observable quantity. With the help of the wave function (5) the expectation value of the dipole operator (15) can be written as:

$$\left\langle D(t)\right\rangle = d_{11}\left|a_1(t)\right|^2 + d_{22}\left|a_2(t)\right|^2$$

$$+ \left\{d_{12}a_1^*a_2\sum_k J_k\left(Z\right)e^{i(k-n)\omega_0 t} + \text{c.c.}\right\}. \qquad (16)$$

where $a_{1,2}(t) = \overline{a}_{1,2}(t) + \alpha_{1,2}(t)$. Combining Eqs. (6), (11), (12), and (16) one can calculate analytically the expectation value of the dipole operator for an arbitrary initial atomic state. The Fourier transform of $\left\langle D(t)\right\rangle$ gives the coherent part of the dipole spectrum.

The solution (6) for the system initially situated in the ground state, is:

$$\overline{a}_1(t) = e^{i\delta_n t/2}\left[\cos\left(\frac{\Omega_n t}{2}\right) - i\frac{2\Delta_n + \delta_n}{\Omega_n}\sin\left(\frac{\Omega_n t}{2}\right)\right], \qquad (17)$$

$$\overline{a}_2(t) = i\frac{2F_n}{\Omega_n}e^{i\delta_n t/2}\sin\left(\frac{\Omega_n t}{2}\right), \qquad (18)$$

which expresses the Rabi oscillations with frequency

$$\Omega_n \equiv \sqrt{4F_n^2 + (2\Delta_n + \delta_n)^2}. \qquad (19)$$

The generalized Rabi frequency at n-photon resonance has nonlinear dependence on the amplitude of a pump wave field. As we can see from (17), (18) the amplitudes of Rabi oscillations are diminished due to dynamic Stark effect. The destructive effect of the latter can be compensated by an appropriate detuning:

$$\delta_n = -2\Delta_n. \qquad (20)$$

Replacing the probability amplitudes in (16) by the corresponding expressions (17) and (18), one can derive the final analytical expression for $\left\langle D(t)\right\rangle$. As is seen from Eqs. (8), (9), the multiphoton coupling is proportional to the ratio d_{12}/d_p, while the dynamic Stark shift is proportional to d_{12}^2/d_p^2. Since large dynamic Stark shifts make difficult the maintenance of considerable population transfer, here we consider systems with $\mu = |d_{12}|/d_p << 1$. Taking into account the smallness of the parameter μ, from (16) in the first order of approximation by the small parameter μ we obtain the following compact analytic formula:

$$\left\langle D(t)\right\rangle = C_0 + \sum_{k\neq 0}[S_k\sin(k\omega_0 t) + C_k\cos(k\omega_0 t)], \qquad (21)$$

where

$$C_0 = d_{11} + \left(d_p\frac{2F_n^2}{\Omega_n^2} - d_{12}\frac{2F_n}{\Omega_n}\frac{2\Delta_n + \delta_n}{\Omega_n}J_n\left(Z\right)\right)$$

$$\times(1 - \cos(\Omega_n t)), \qquad (22)$$

describes the low-frequency part of the spectrum, and

$$S_k = d_{12}\frac{2F_n}{\Omega_n}\frac{nJ_{n+k}\left(Z\right)}{k}\sin(\Omega_n t), \qquad (23)$$

$$C_k = d_{12}\frac{2F_n}{\Omega_n}\frac{2\Delta_n + \delta_n}{\Omega_n}\frac{nJ_{n+k}\left(Z\right)}{k}(1 - \cos(\Omega_n t)), \qquad (24)$$

describe harmonic radiation. As we can see from (23)-(24), the harmonic spectrum consists of triplets, with harmonic and two hyper-Raman lines with frequencies displaced by Ω_n. From (19) follows that frequencies of hyper-Raman and low-frequency lines can be smoothly tuned via variation of the laser field strength and detuning.

The expression for $\left\langle D(t)\right\rangle$ shows that intensities of the harmonics mainly determined by the behaviour of Bessel function. Since the Bessel function $J_m\left(Z\right)$ steeply decreases with increase of index $m \gtrsim Z$, then the cut-off harmonic s_c is determined from the condition $s_c - n \sim Z$. Then, from the estimation for cut-off harmonic follows that upper limit of the frequency which can be effectively generated by direct n-photon excitation, is higher for the systems with larger difference of energy and dipole moments in stationary states ($\omega_c \sim \varepsilon_2 - \varepsilon_1 + d_p E_0$). Although cut-off frequency is not directly depend on the
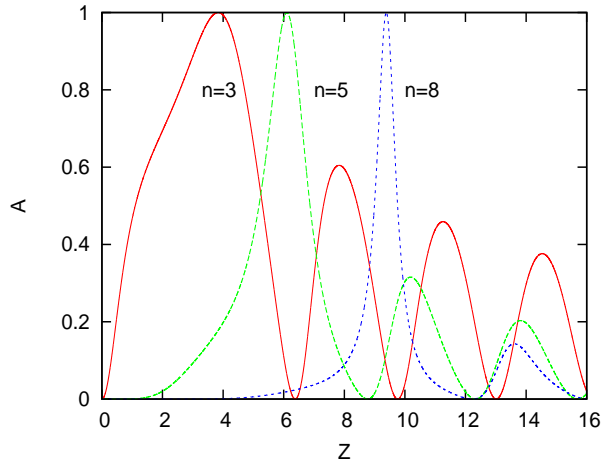
FIG. 1: (Color online) The dependence of the amplitude of state-populations oscillation $A = 4F_n^2/\Omega_n^2$ on parameter Z for zero detuning ($\delta_n = 0$) and $d_{12}/d_p = 0.1$. The solid (red) line corresponds to the three-photon ($n = 3$) resonance; the dashed (green) line corresponds to the five-photon ($n = 5$) resonance; the dotted (blue) line corresponds to the eight-photon ($n = 8$) resonance.

photon order n of the resonance, but taking into account harmful ionization, the large n is preferred for efficient harmonic generation at the given strength of the laser field. Note that due to the oscillating character of Bessel function, harmonics can be strengthened or weakened via variation of the laser field strength within the resonance width.

The intensity of the harmonic components is proportional to F_n^2/Ω_n^2, which is the amplitude of population oscillations of the states. Thus, for the effective radiation generation one should provide a considerable population transfer between the ground and excited states, i.e., $|F_n| \sim \Omega_n$. As it follows from (8), (9), and (19), besides the ratio d_{12}/d_p, parameter Z may also have substantial effect on population transfer. In Fig. 1 we plot dependence of the amplitude of population oscillations of the states on parameter Z, for zero detuning and different values of the photon order n. The complete population transfer is achieved when $\Delta_n = 0$. In fact, for considerable population transfer it is important to compensate dynamic Stark shift by an appropriate detuning, specifically for high-order multiphoton excitation in the weaker laser fields.

The pattern of dipole intensities in harmonic triplet is determined from the expressions (23)-(24):

$$\frac{I_{k\omega_0 \pm \Omega_n}}{I_{k\omega_0}} = \frac{1}{4}\left[\frac{J_{n-k}(Z) + J_{n+k}(Z)}{J_{n-k}(Z) - J_{n+k}(Z)}\frac{\Omega_n}{2\Delta_n + \delta_n} \mp 1\right]^2. \tag{25}$$

In general, due to oscillating character of the Bessel functions, the triplet pattern can be significantly changed depending on the pump wave field strength. In moderately strong laser fields $Z \lesssim 1$ and in case of considerable population transfer, i.e., when $\Omega_n \simeq |2\Delta_n + \delta_n|$, one of the

hyper-Raman lines becomes weaker than the other two lines of the triplet. Distribution of intensities is essentially changed for almost complete population transfer, i.e., when $\Omega_n \approx 2|F_n| \gg |2\Delta_n + \delta_n|$. In this case the intensities of the hyper-Raman components become on the same order and harmonic component practically vanishes. The latter is proportional to μ^2 and appears only in the next order of approximation by the small parameter μ.

C. LOW-FREQUENCY RADIATION

As it has been mentioned above, the expectation value of the dipole operator (21) also has low-frequency term $\langle D_{\text{low}}(t)\rangle$ which is given by the formula:

$$\langle D_{\text{low}}(t)\rangle = -d_p\left[\frac{2F_n^2}{\Omega_n^2} - \frac{d_{12}}{d_p}\frac{2F_n}{\Omega_n}\right.$$

$$\left.\times\frac{2\Delta_n + \delta_n}{\Omega_n}J_n(Z)\right]\cos\left(\Omega_n t\right), \tag{26}$$

according to Eq. (22). Formula (26) describes the radiation at the smoothly tunable frequency Ω_n, i.e., at the frequency of oscillations of the population inversion. This low-frequency radiation also depends on the amplitude of population oscillations of the states. According to Eq. (26), with increase of the amplitude of Rabi oscillations the intensity of low-frequency radiation increases. When population transfer is almost complete, e.g., when dynamic Stark shift is compensated by appropriate detuning, the low-frequency term can be written as:

$$\langle D_{\text{low}}(t)\rangle = -\frac{d_p}{2}\cos(\Omega_R t), \tag{27}$$

where the Rabi frequency Ω_R is determined by the expression:

$$\Omega_R = \left|2\frac{d_{12}}{d_p}n\omega_0 J_n(Z)\right|. \tag{28}$$

In this case the emitted radiation intensity does not depend on the pump wave field strength and is determined only by the difference of PDM in the excited and ground states.

For the considered problem, the Rabi frequency may be varied within the following limits: $2\pi/T_r << \Omega_R << \omega_0$, where T_r describes the relaxation time in the molecular system. Hence, for electronic transitions Ω_R can lie from microwave to infrared frequencies. Here, we concentrate on terahertz region of electromagnetic spectrum ($0.1 - 10$ THz) due to the important properties of such radiation and its numerous applications for spectroscopy, sensing, imaging, and etc (for a review see [27]).

For comparison of considered scheme with the other schemes of THz radiation, we make some estimations for

total radiation power of the ensemble of N molecular emitters. It is assumed that the molecules are oriented in the same direction. Though, in case of freely rotating molecules temperature-dependent distribution of molecular orientations reduces transition and permanent dipole moments, the intensity of emitted radiation also will be reduced to some extent. Due to phase-matching factor the coherent radiation entirely occurs almost in forward direction. The power of low-frequency radiation was evaluated for resonantly driven three-level atomic-molecular ensemble in [16] and will not be repeated here in detail. We will adopt the estimations made for circular cylinder model of superradiant emitter (in a limit of long needle) for ensemble of 2-level polar molecules. The radiation power for ensemble of polar molecules coherently excited by Gaussian laser beam with a waist w_0 can be approximated by formula:

$$P \simeq \frac{d_p^2 \Omega_R^3}{16c^2} \frac{\pi^3 w_0^4}{n^2} \Delta_\Omega^2 L_c N_0^2, \qquad (29)$$

where Δ_Ω is a degree of monochromaticity specified by driven field variation in the interaction region, L_c is the coherent length over which the low-frequency can be built up coherently and N_0 is the density of polar emitters. The corresponding incident pulse duration should be: $\tau \gtrsim 2\pi n/(\Omega_R \Delta_\Omega)$. As we can see from (29), it is more desirable to generate THz radiation via low-order multiphoton excitation. Here we make estimations for two-photon resonance ($n = 2$); the incident laser beam waist is taken to be: $w_0 \gtrsim 1$ mm, the coherence length: $L_c \gtrsim 10$ cm, the difference of PDM in the excited and ground states: $d_p \sim 5$ a.u. and emitters density: $N_0 \sim 10^{15}$ cm^{-3}. For the moderate monochromaticity $\Delta_\Omega = \delta\Omega_R/\Omega_R \sim 0.1$ at $\Omega_R/(2\pi) \simeq 3$ THz, the incident pulse duration should be: $\tau \gtrsim 6$ ps. Estimated total radiation power $P \simeq 100$ W is comparable with parameters for most powerful THz sources. Note that submillimeter-sized array of resonantly driven 2-level quantum dots with induced dipole moment ~ 10 D gives the power of microwatt level [15].

In case of a solid medium, the radiation power could be larger due to higher densities of matter. The other advantage of the solid medium is the degree of anisotropy, since molecules can practically be oriented in the same direction, e.g., in some organic crystals or when the molecules are inserted in a solid matrix that is transparent to the radiation. The volume of coherent radiation for a solid medium is $\sim \lambda^3$, and the number of polar emitters can be estimated by $N \sim \lambda^3 N_0$, which at densities $N_0 \sim 10^{21}$ cm^{-3} gives $N \sim 10^{15}$. The rough estimations show that using submillimeter-sized crystals with $\sim 1\%$ ordered dipole moments of emitters one can achieve giant total radiation power for coherent THz radiation up to megawatt level.

III. NUMERICAL RESULTS AND DISCUSSION

In this section we present numerical solutions of time-dependent Schrödinger equation for a two-level model with Hamiltonian (1). The set of equations for the probability amplitudes has been solved using a standard fourth-order Runge-Kutta algorithm [28]. The Fourier transformations for estimation of power spectra are performed using the fast Fourier transform technique. For smooth turn-on of pump wave field, the latter is described by the envelope in hyperbolic tangent $\tanh(t/\tau)$ form, where τ characterizes the turn-on time and chosen to be $20\pi/\omega_0$. The transition frequency is set to be $\varepsilon_2 - \varepsilon_1 = 0.2$ a.u. and lies in UV region, but the results can be scaled to different energy regimes. The transition dipole moment is chosen to be $d_{12} = 0.5$ a.u., and difference of PDM in the excited and ground states: $d_p = 5$ a.u. (except where it is declared otherwise). It is assumed that initially all the population is in the ground state $|1\rangle$.

Figure 2 shows dipole spectrum (coherent part) as a function of harmonic order for four-photon ($n = 4$) resonant excitation. The pump field strength is $E = 0.01$ a.u. and multiphoton detuning δ_n is set to zero. The solid (red) line corresponds to numerical calculations, while the dashed (green) line corresponds to the approximate expression (21). For better visibility, the spectrum corresponding to analytical calculations has been slightly shifted to the right. As we can see from the Fig. 2, the analytical formula (21) is in good agreement with the exact results. For employed field strengths the triplet structure of harmonics and low-frequency line are not clearly seen, hence the latter is illustrated in the inset.

Dipole spectrum as a function of harmonic order for five-photon ($n = 5$) resonant excitation with almost complete population transfer is plotted in Fig. 3. The pump field strength is $E = 0.01$ a.u. and detuning for compensation of dynamic Stark shift is $\delta_n = 0.00014$ a.u.. As in Fig 2, the solid (red) line corresponds to numerical calculations and the dashed (green) line corresponds to the approximate expression (21). The numerical results confirm the analytical expression for expectation value of the mean dipole moment. These figures confirm the estimation $s_c - n \sim Z$ for cut-off position.

In Fig. 4 we plot characteristic harmonic triplet (here, for 6th harmonic) under the same conditions of excitation, as in Fig. 3. The solid (red) line corresponds to detuning, compensating dynamic Stark shift, and dashed (green) line corresponds to zero detuning. For better visibility, the spectrum corresponding to compensating detuning has been slightly shifted to the right. The numerical results confirm estimations for lines position in harmonic triplet and the fact that via compensation of dynamic Stark shifts one can attain the higher intensities. Distribution of intensities, particularly, damping of harmonic lines in case of compensating detuning and lower-frequency hyper-Raman lines at zero detuning, have been predicted in section II.
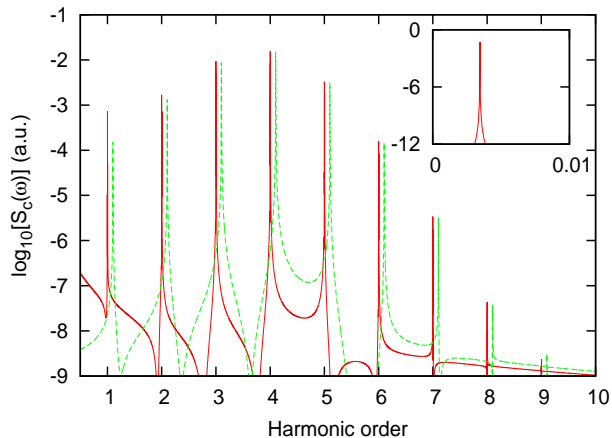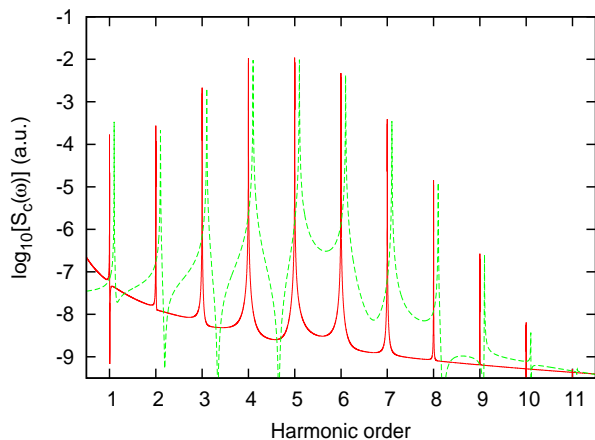
FIG. 2: (Color online) The logarithm of the coherent part of the spectrum $S_C(\omega)$ at four-photon ($n = 4$) resonance with zero detuning ($\delta_n = 0$). The energy level difference is $\varepsilon_2 - \varepsilon_1 = 0.2$ a.u., laser field strength $E = 0.01$ a.u., and dipole moments are $d_{12} = 0.5$ a.u. and $d_p = 5$ a.u.. The solid (red) line corresponds to numerical calculations; the dashed (green) line corresponds to the approximate solution (for better visibility the latter has been slightly shifted to the right). The inset shows the low-frequency peak at Rabi frequency.

FIG. 3: (Color online) The logarithm of the coherent part of the spectrum $S_C(\omega)$ at five-photon ($n = 5$) resonance. The energy level difference is $\varepsilon_2 - \varepsilon_1 = 0.2$ a.u., detuning $\delta_n = 0.00014$ a.u., laser field strength $E = 0.01$ a.u., and dipole moments are $d_{12} = 0.5$ a.u. and $d_p = 5$ a.u.. The solid (red) line corresponds to numerical calculations; the dashed (green) line corresponds to the approximate solution (for better visibility the latter has been slightly shifted to the right).

To demonstrate the effects of PDM we plot the spectrum of the two-level system without PDM under the same conditions of excitation, as in Fig. 3. As is shown in Fig. 5, there are fewer harmonics and with negligibly small amplitudes. Practically the full radiation is concentrated on the incident radiation frequency. Even harmonics, as well as the low-frequency radiation are absent because of inversion symmetry. Note that these essen-
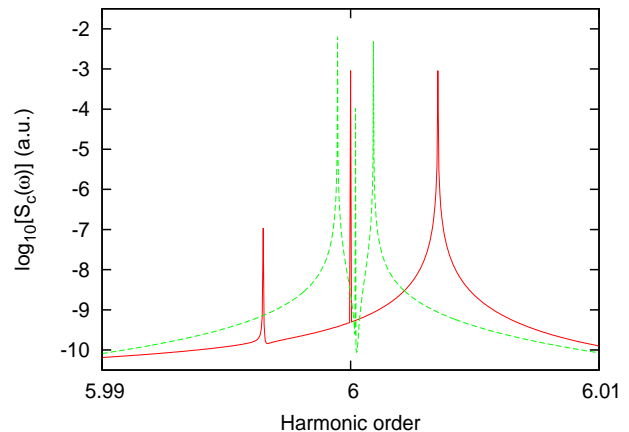

FIG. 4: (Color online) The structure of satellite peaks around the 6th harmonics under the same conditions of excitation as in Fig. 2. The solid (red) line corresponds to zero detuning ($\delta_n = 0$); the dashed (green) line corresponds to detuning $\delta_n = 0.00014$ a.u. (for better visibility the latter has been slightly shifted to the right).
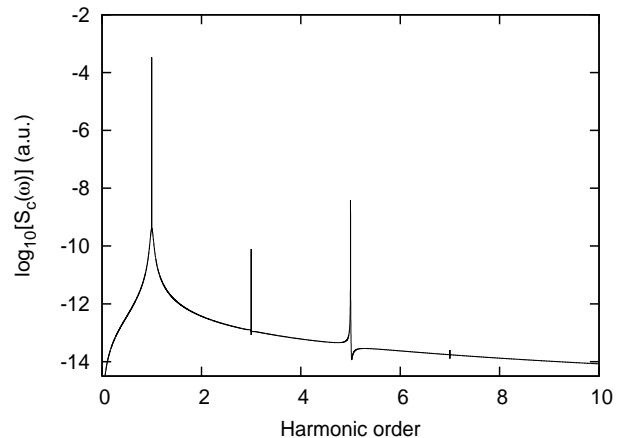

FIG. 5: Same as in figure 2, but for the case of zero dipole moments in stationary states.

tial distinctions in intensities of the harmonics are for the pump field strengths with negligible ionization and dynamic Stark shifts. To achieve the efficient harmonic generation when $d_p = 0$, required laser fields should be comparable to characteristic fields of considered system: $E_0 \gtrsim (\varepsilon_2 - \varepsilon_1) / d_{12}$, which will cause complete ionization.

We also made numerical calculations for low-frequency part of the radiation spectrum. Figure 6 displays the dependence of the emission rate on emission frequency at five-photon resonance. The lower line corresponds to zero detuning and upper line to detuning compensating dynamic Stark shift. The calculations have been made for the same field strengths. As we can see from the Fig. 6, the frequency and intensity of the emission lines appreciably depend on the magnitude of the detuning and
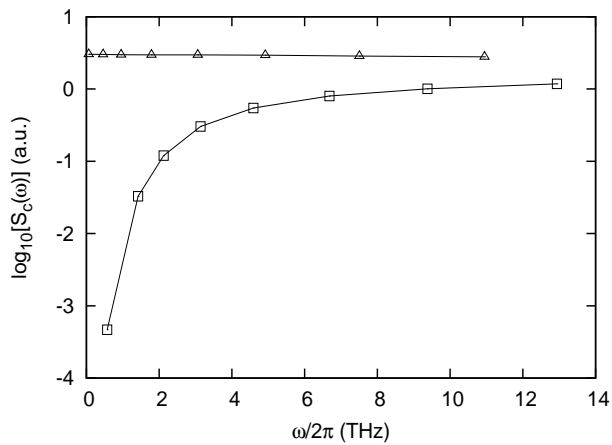
FIG. 6: The low-frequency emission rate as a function of the emission frequency under the same conditions of excitation as in Fig. 2. (a) upper line corresponds to compensated dynamic Stark shift. (b) lower line corresponds to zero detuning ($\delta_n = 0$).

compensation of the Stark shift is of considerable importance. The numerical results for spectral characteristics are in good agreement with estimations based on (26) and (27).

It should be noted that evenly charged molecular ions at large internuclear distances [11], driven flux qubits [29], and hydrogenlike atoms [10, 12, 13] are good examples of efficient direct multiphoton excitation. The mentioned three-level configurations are also good candidates for moderately high harmonics generation [6]. However, in contrast to 2-level model with PDM, due to inversion symmetry the spectrum of three-level system does not contain even harmonics (with corresponding hyper-Raman lines) and low-frequency components under the conditions of excitation considered here.

IV. CONCLUSION

We have presented a theoretical treatment of the dipole spectrum of a two-level system possessing PDM under direct multiphoton resonant excitation. With the help of nonperturbative resonant approach, we have studied approximate stationary solution of the Schrodinger equation and obtain a simple analytical expression for scattered coherent radiation. We have also numerically investigated the harmonic spectra and effects of compensation of the dynamic Stark shift on emission spectrum. As has been shown, the compensation of dynamic Stark shift by appropriate detuning could substantially improve efficiency of radiation generation. The numerical results are in good agreement with obtained analytical results for expectation value of dipole operator. We have also shown that the existence of PDM enables the considerable population transfer in moderately strong laser fields, and therefore could contribute to generation of higher harmonics with sufficiently large amplitudes. In addition, due to broken inversion symmetry of systems with PDM there is substantial emission at frequency much smaller than the laser frequency. The considered scheme may serve as a promising method for efficient generation of moderately high harmonics and intense widely tunable low-frequency radiation. Note that for coherent radiation of an molecular ensemble one needs more rigorous treatment, which should account for degree of anisotropy in the orientational distribution of polar molecules, as well as collective effects in the medium. Work in this direction is in progress and will be presented in forthcoming paper.

[1] B. W. Shore and P. L. Knight, J. Phys. B **20**, 413 (1987); P. B. Corkum, Phys. Rev. Lett. **71**, 1994 (1993); M. Lewenstein, Ph. Balcou, M. Yu. Ivanov, A. L'Huillier, and P.B. Corkum, Phys. Rev. A **49**, 2117 (1994).

[2] M. Protopapas, C. H. Keitel, and P. L. Knight, Rep. Prog. Phys. **60**, 389 (1997); P. Saliéres A. L'Huillier, P. Antoine, and M. Lewenstein, Adv. At., Mol., Opt. Phys. **41**, 83 (1999); T. Brabec and F. Krausz, Rev. Mod. Phys. **72**, 545 (2000); P. Agostini and L. F. DiMauro, Rep. Prog. Phys. **67**, 813 (2004).

[3] P. Haljan, T. Fortier, P. Hawrylak, P. B. Corkum, and M. Yu. Ivanov, Laser Phys. **13**, 452 (2003); D. Golde, T.

Meier, and S.W. Koch, Phys. Rev. B **77**, 075330 (2008).

[4] Z. H. Kafafi, J. R. Linde, R. G. S. Pong, F. J. Bartoli, L. J. Lingg, and J. Milliken, Chem. Phys. Lett. **188**, 492 (1992); G.P. Zhang, Phys. Rev. Lett. **95**, 047401 (2005).

[5] V. Averbukh, O. E. Alon, and N. Moiseyev, Phys. Rev. A **64**, 033411 (2001); C. F. deMorissonFaria and I. Rotter, Phys. Rev. A **66**, 013402 (2002).

[6] H. K. Avetissian, B. R. Avchyan, and G. F. Mkrtchian, Phys. Rev. A **77**, 023409 (2008).

[7] V. P. Krainov and Z. S. Milyukov, Laser Phys. **4**, 544 (1994).

[8] R. E. Duvall, E. J. Valeo, and C. R. Oberman, Phys.

Rev. A **37**, 4685 (1988).

[9] M. A. Kmetic and W. J. Meath, Physics Letters A **108**, 340 (1984); A. Brown, W. J. Meath, and P. Tran, Phys. Rev. A **63**, 013403 (2000); *ibid.* **65**, 063401 (2002).

[10] H. K. Avetissian and G. F. Mkrtchian, Phys. Rev. A **66**, 033403 (2002).

[11] G. N. Gibson, Phys. Rev. Lett. **89**, 263001 (2002).

[12] H. K. Avetissian, G. F. Mkrtchian, M. G. Poghosyan, Phys. Rev. A **73**, 063413 (2006).

[13] H. K. Avetissian, B.R. Avchyan, G. F. Mkrtchian, Phys. Rev. A **74**, 063413 (2006).

[14] H. K. Avetissian, A. Brown, G. F. Mkrtchian, Phys. Rev. A **80**, 033413 (2009).

[15] O. V. Kibis, G. Y. Slepyan, S. A. Maksimenko, and A. Hoffmann, Phys. Rev. Lett. **102**, 023601 (2009).

[16] H. K. Avetissian, B. R. Avchyan, and G. F. Mkrtchian, Phys. Rev. A **82**, 063412 (2010).

[17] O. G. Calderón, R. Gutiérrez-Castrejón, and J. M. Guerra, IEEE J. Quantum Electron. **35**, 47 (1999).

[18] V. P. Gavrilenko and E. Oks, J. Phys. B **33**, 1629 (2000).

[19] D. L. Andrews and W. J. Meath, J. Phys. B **26**, 4633 (1993).

[20] A. Brown and W. J. Meath, Phys. Rev. A **53**, 2571 (1996).

[21] S. H. Nilar, A. J. Thakkar, A. E. Kondo, and W. J. Meath, Can. J. Chem. **71**, 1663 (1993).

[22] V. A. Kovarskii, Phys. Usp. **42**, 797 (1999).

[23] D. A. Telnov and Shih-I Chu, Phys. Rev. A **71**, 013408 (2005); A. D. Bandrauk, S. Chelkowski, D. J. Diestler, J. Manz, and K.-J. Yuan, Phys. Rev. A **79**, 023403 (2009).

[24] G. N. Watson, *A Treatise on the Theory of Bessel Functions* (Cambridge University Press, Cambridge, 1944).

[25] J. H. Eberly and M. V. Fedorov, Phys. Rev. A **45**, 4706 (1992).

[26] D. G. Lappas, M. V. Fedorov, and J. H. Eberly, Phys. Rev. A **47**, 1327 (1993).

[27] P. H. Siegel, IEEE Trans. Microw. Theory Tech., **50**, 910 (2002); D. Mittleman, *Sensing with Terahertz Radiation*, (Springer, Heidelberg, 2003); D. Dragoman and M. Dragoman, Progress in Quantum Electronics **28**, 1 (2004); D. W. Woolard, E. R. Brown, M. Pepper, and M. Kemp, Proc. IEEE **93**, 1722 (2005); M. Tonouchi, Nature Photonics **1**, 97 (2007).

[28] W. H. Press, S. A. Teukolsky, W. T. Vetterling, and B. P. Flannery, *Numerical Recipes in C* (Cambridge University Press, Cambridge, 1992).

[29] W. D. Oliver, Y. Yu, J. C. Lee, K. K. Berggren, L. S. Levitov, and T. P. Orlando, Science **310**, 1653 (2005).